

Practical design of a nonlinear tuned vibration absorber

C. Grappasonni¹, G. Habib¹, T. Detroux¹, F. Wang², G. Kerschen¹, J.S. Jensen³

¹ University of Liège, Department of Aerospace and Mechanical Engineering
Chemin des chevreuils 1 B52, B-4000, Liège, Belgium
e-mail: chiara.grappasonni@ulg.ac.be

² Technical University of Denmark, Department of Mechanical Engineering
Nils Koppels Allé B404, 2800, Kgs. Lyngby, Denmark

³ Technical University of Denmark, Department of Electrical Engineering
Ørsteds Plads B352, 2800, Kgs. Lyngby, Denmark

Abstract

The aim of the paper is to develop a new nonlinear tuned vibration absorber (NLTVA) capable of mitigating the vibrations of nonlinear systems which are known to exhibit frequency-energy-dependent oscillations. A nonlinear generalization of Den Hartog's equal-peak method is proposed to ensure equal peaks in the nonlinear frequency response for a large range of forcing amplitudes. An analytical tuning procedure is developed and provides the load-deflection characteristic of the NLTVA. Based on this prescribed relation, the NLTVA design is performed by two different approaches, namely thanks to (i) analytical formulas of uniform cantilever and doubly-clamped beams and (ii) numerical shape optimization of beams with varying width and thickness. A primary system composed of a cantilever beam with a geometrically nonlinear component at its free end serves to illustrate the proposed methodology.

1 Introduction

Vibration mitigation offers the possibility of improving the performance, comfort or safety of a mechanical system. Real-life applications often exhibit resonant vibrations, which can be exacerbated for nonlinear structures, at least in specific operating regimes. Expanding the performance envelope of such engineering systems is the aim of the present study. Many attempts for vibration reduction around one resonance using linear and nonlinear absorbers have been suggested in the literature. Passive linear absorbers are optimal in case of linear primary structures. Den Hartog's equal-peak method provides a widely-used design strategy based on approximate analytical formulas for the absorber stiffness and damping [1, 2, 3]. Interestingly, an exact closed-form solution for this classical problem was found only almost 100 years later [4]. Nevertheless, this solution is only valid for undamped linear primary systems. The introduction of linear damping complicates further the problem, and Asami et al. [5] proposed the series solution adopted in this paper for minimizing the maximal frequency response.

However, linear absorbers suffer from a narrow bandwidth and cannot effectively damp out the vibrations of nonlinear systems, which are known to exhibit frequency-energy-dependent oscillations. Nonlinear vibration absorbers, including the autoparametric vibration absorber [6] and the nonlinear energy sink (NES) [7] can absorb disturbances in wider ranges of frequencies due to their increased bandwidth. However, the performance of existing nonlinear vibration absorbers is known to exhibit marked sensitivity to motion amplitudes. For instance, there exists a well-defined threshold of input energy below which no significant energy dissipation can be induced in an NES [7]. Likewise, the saturation phenomenon characteristic of autoparametric vibration absorbers occurs only when the forcing amplitude exceeds a certain threshold [6]. In

this paper, a nonlinear tuned vibration absorber (NLTVA) is introduced to mitigate a specific nonlinear resonance of the main structure in wide ranges of motion amplitudes. The basic idea develops from Den Hartog’s method, which is extended to ensure equal peaks in the nonlinear frequency response. The linear parameters of the NLTVA are selected according to Asami’s solution [5], and the absorber’s nonlinear load-deflection characteristic is tailored according to the nonlinear restoring force of the host structure.

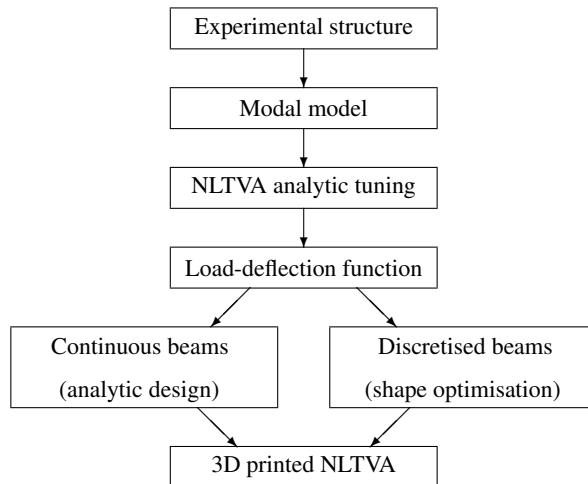


Figure 1: Diagram of the design procedure.

The practical design of the NLTVA proposed in the present work is summarised in Figure 1. Starting from a previously-characterized experimental structure, an equivalent single-degree-of-freedom (SDOF) modal model of the targeted resonance is first derived. From the modal model, an analytical tuning procedure provides the absorbers’ parameters, and, in particular, its load-deflection characteristic. The practical implementation of the NLTVA is achieved using straight geometrically nonlinear beams with cantilever or doubly-clamped boundary conditions. Based on the prescribed load-deflection curve, the design of these beams is then performed by two different approaches based on either continuous or discretised beam models. The former approach utilises existing analytical formulas of uniform beams whereas the latter approach involves numerical shape optimisation of beams with varying width and thickness. Finally, these optimized designs can be fabricated using 3D printers.

2 Nonlinear generalization of the equal-peak method

2.1 The linear tuned vibration absorber (LTVA)

The steady-state response of an undamped mass-spring system subjected to a harmonic excitation at a constant frequency can be suppressed using an undamped linear tuned vibration absorber (LTVA), as proposed by Frahm in 1909 [9]. However, the LTVA performance deteriorates significantly when the excitation frequency varies. To improve the performance robustness, damping was introduced in the absorber by Ormondroyd and Den Hartog [2]. The equations of motion of the coupled system are

$$\begin{aligned}
 m_1\ddot{x}_1 + k_1x_1 + c_2(\dot{x}_1 - \dot{x}_2) + k_2(x_1 - x_2) &= F \cos \omega t \\
 m_2\ddot{x}_2 + c_2(\dot{x}_2 - \dot{x}_1) + k_2(x_2 - x_1) &= 0
 \end{aligned} \tag{1}$$

where $x_1(t)$ and $x_2(t)$ are the displacements of the harmonically-forced primary system and of the damped LTVA, respectively. Den Hartog realized that the receptance function of the primary mass passes through two invariant points independent of absorber damping. He proposed to adjust the absorber stiffness to have

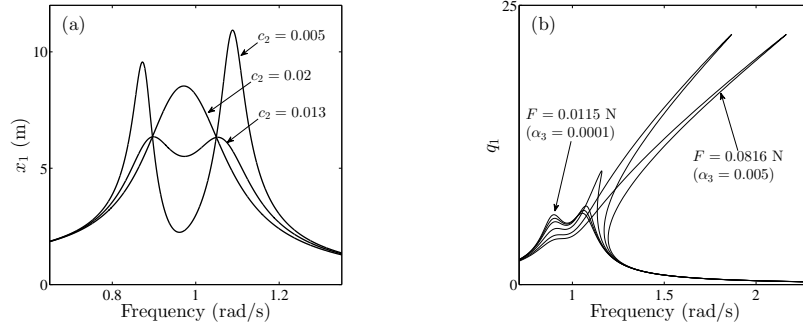


Figure 2: (a) Illustration of Den Hartog's equal-peak method, $\epsilon = 0.05$ and $k_2 = 0.0454$ N/m. (b) Frequency response of a Duffing oscillator with an attached LTVA. q_1 is the dimensionless amplitude ($q_1 = x_1 k_1 / F$). For the computation $m_1 = 1$ kg, $c_1 = 0.002$ Ns/m ($\mu_1 = 0.001$), $k_1 = 1$ N/m, $k_{nl1} = 1$ N/m³ and $\epsilon = 0.05$. For the different curves $F = 0.0115$ N, $F = 0.0258$ N, $F = 0.0365$ N, $F = 0.0577$ N, and $F = 0.0816$ N ($\alpha_3 = 0.0001$, $\alpha_3 = 0.0005$, $\alpha_3 = 0.001$, $\alpha_3 = 0.0025$ and $\alpha_3 = 0.005$, see later), where F is the forcing amplitude.

two fixed points of equal heights in the receptance curve and to select the absorber damping so that the curve presents a horizontal tangent through one of the fixed points. This laid down the foundations of the so-called equal-peak method. Den Hartog [1] and Brock [3] derived approximate analytical formulas for the absorber stiffness and damping, respectively. Interestingly, an exact closed-form solution for this classical problem was found only ten years ago [4].

The introduction of linear damping into the primary system complicates further the problem, because of the disappearance of the invariant points; a series solution for minimizing the maximal frequency response was proposed in [5]:

$$\begin{aligned} \lambda &= \frac{\omega_{n2}}{\omega_{n1}} = \sqrt{\frac{k_2 m_1}{k_1 m_2}} = \frac{1}{1 + \epsilon} - \mu_1 \frac{1}{1 + \epsilon} \sqrt{\frac{1}{2(1 + \epsilon)}} \left(3 + 4\epsilon - \frac{AB}{2 + \epsilon} \right) + \mu_1^2 \frac{C_0 - 4(5 + 2\epsilon)AB}{4(1 + \epsilon)^2(2 + \epsilon)(9 + 4\epsilon)} \\ \mu_2 &= \frac{c_2}{2\sqrt{k_2 m_2}} = \sqrt{\frac{3\epsilon}{8(1 + \epsilon)}} + \mu_1 \frac{60 + 63\epsilon + 16\epsilon^2 - 2(3 + 2\epsilon)AB}{8(1 + \epsilon)(2 + \epsilon)(9 + 4\epsilon)} + \\ &\quad \mu_1^2 \frac{C_1(A + B)\sqrt{2 + \epsilon} + C_2(A - B)\sqrt{\epsilon}}{32(1 + \epsilon)(2 + \epsilon)^2(9 + 4\epsilon)^3\sqrt{2\epsilon(1 + \epsilon)}} \end{aligned} \quad (2)$$

where

$$\begin{aligned} A &= \sqrt{3(2 + \epsilon) - \sqrt{\epsilon(2 + \epsilon)}}, \quad B = \sqrt{3(2 + \epsilon) + \sqrt{\epsilon(2 + \epsilon)}} \\ C_0 &= 52 + 41\epsilon + 8\epsilon^2 \\ C_1 &= -1296 + 2124\epsilon + 6509\epsilon^2 + 5024\epsilon^3 + 1616\epsilon^4 + 192\epsilon^5 \\ C_2 &= 48168 + 112887\epsilon + 105907\epsilon^2 + 49664\epsilon^3 + 11632\epsilon^4 + 1088\epsilon^5 \end{aligned} \quad (3)$$

ω_{n1} and ω_{n2} are the natural frequencies of the primary system and of the absorber, respectively, $\epsilon = m_2/m_1$ is the mass ratio, $\mu_1 = c_1/(2\sqrt{k_1 m_1})$ and μ_2 are the damping ratio of the primary system and of the absorber, respectively. For $m_1 = 1$ kg, $k_1 = 1$ N/m, $c_1 = 0.002$ Ns/m and $\epsilon = 0.05$, the equal-peak method yields $\lambda = 0.952$ and $\mu_2 = 0.134$, and, hence, $k_2 = 0.0454$ N/m and $c_2 = 0.0128$ Ns/m. As illustrated in Fig. 2 (a), this tuning condition minimizes the maximum response amplitude of the primary system. It is still widely used, as discussed in the review paper [10].

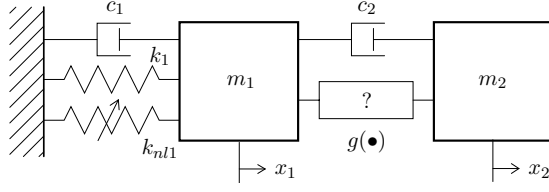


Figure 3: Schematic representation of an NLTVA attached to a Duffing oscillator.

2.2 LTVA coupled to a Duffing oscillator

Considering a harmonically-forced, lightly-damped Duffing oscillator as primary system, the performance of the LTVA attached to this nonlinear system is investigated.

Figure 2 (b) shows the displacement response of the primary mass with an attached LTVA for various forcing amplitudes F , whose equations of motion are

$$\begin{aligned} m_1 \ddot{x}_1 + c_1 \dot{x}_1 + k_1 x_1 + k_{nl1} x_1^3 + c_2 (\dot{x}_1 - \dot{x}_2) + k_2 (x_1 - x_2) &= F \cos \omega t \\ m_2 \ddot{x}_2 + c_2 (\dot{x}_2 - \dot{x}_1) + k_2 (x_2 - x_1) &= 0. \end{aligned} \quad (4)$$

The frequency response curves were computed using a path-following algorithm combining shooting and pseudo-arclength continuation. The algorithm is similar to that used in [11]. In the figure it is seen that for low values of forcing amplitude F , the two resonant peaks have similar amplitude. However, increasing the forcing amplitude and practically activating the nonlinearity of the system, there is a clear detuning of the LTVA, i.e. the amplitude of one resonant peak is increased significantly making the absorber ineffective.

2.3 The nonlinear tuned vibration absorber (NLTVA)

In view of the results presented in the previous section, it is meaningful to examine the performance of nonlinear absorbers for vibration mitigation of nonlinear primary structures. Roberson was the first to observe a broadening of the suppression band through the addition of a nonlinear spring that he chose to be cubic for facilitating its practical realization [12]. However, as pointed out in the introductory section, this increased bandwidth may come at the price of a marked sensitivity to external forcing amplitude.

To mitigate a nonlinear resonance in an as large as possible range of forcing amplitudes, we introduce the nonlinear tuned vibration absorber (NLTVA). One unconventional feature of this absorber is that the mathematical form of its nonlinear restoring force is not imposed a priori, as it is the case for most existing nonlinear absorbers. Instead, we propose to fully exploit the additional design parameters offered by nonlinear devices and, hence, to synthesize the absorber's load-deflection curve according to the nonlinear restoring force of the primary structure.

The dynamics of a Duffing oscillator with an attached NLTVA as depicted in Fig. 3 is considered:

$$\begin{aligned} m_1 \ddot{x}_1 + c_1 \dot{x}_1 + k_1 x_1 + k_{nl1} x_1^3 + c_2 (\dot{x}_1 - \dot{x}_2) + g(x_1 - x_2) &= F \cos \omega t \\ m_2 \ddot{x}_2 + c_2 (\dot{x}_2 - \dot{x}_1) - g(x_1 - x_2) &= 0 \end{aligned} \quad (5)$$

The NLTVA is assumed to have a generic smooth restoring force $g(x_1 - x_2)$ with $g(0) = 0$. After the definition of the dimensionless time $\tau = \omega_{n1} t$, where $\omega_{n1} = \sqrt{k_1/m_1}$, the application of the transformation $r(t) = x_1(t) - x_2(t)$ yields

$$\begin{aligned} x_1'' + 2\mu_1 x_1' + x_1 + \frac{4}{3} \tilde{\alpha}_3 x_1^3 + 2\mu_2 \lambda \epsilon r' + \frac{\epsilon}{m_2 \omega_{n1}^2} g(r) &= f \cos \gamma \tau \\ r'' + 2\mu_1 x_1' + x_1 + \frac{4}{3} \tilde{\alpha}_3 x_1^3 + 2\mu_2 \lambda (\epsilon + 1) r' + \frac{\epsilon + 1}{m_2 \omega_{n1}^2} g(r) &= f \cos \gamma \tau \end{aligned} \quad (6)$$

where prime denotes differentiation with respect to time τ , $2\mu_1 = c_1/(m_1\omega_{n1})$, $\tilde{\alpha}_3 = 3/4k_{nl1}/k_1$, $2\mu_2 = c_2/(m_2\omega_{n2})$, $\lambda = \omega_{n2}/\omega_{n1}$, $\epsilon = m_2/m_1$, $f = F/k_1$ and $\gamma = \omega/\omega_{n1}$. We note that ω_{n2} is the linearised frequency of the NLTVA.

Expanding $g(r)$ in Taylor series around $r = 0$ and normalizing the system using $q_1 = x_1/f$ and $q_2 = r/f$, we obtain

$$\begin{aligned} q_1'' + 2\mu_1 q_1' + q_1 + \frac{4}{3}\tilde{\alpha}_3 f^2 q_1^3 + 2\mu_2 \lambda \epsilon q_2' + \lambda^2 \epsilon q_2 + \frac{\epsilon}{m_2 \omega_{n1}^2} \sum_{k=2}^{\infty} \frac{f^{k-1}}{k!} \left. \frac{d^k g}{dr^k} \right|_{r=0} q_2^k &= \cos \gamma \tau \\ q_2'' + 2\mu_1 q_2' + q_2 + \frac{4}{3}\tilde{\alpha}_3 f^2 q_1^3 + 2\mu_2 \lambda (\epsilon + 1) q_2' + \lambda^2 (\epsilon + 1) q_2 + \frac{\epsilon + 1}{m_2 \omega_{n1}^2} \sum_{k=2}^{\infty} \frac{f^{k-1}}{k!} \left. \frac{d^k g}{dr^k} \right|_{r=0} q_2^k &= \cos \gamma \tau \end{aligned} \quad (7)$$

In Eqs. (7), the linear terms are independent of the forcing amplitude f , which confirms that a purely linear absorber attached to a linear oscillator is effective irrespective of the considered forcing amplitude. Focusing now on the complete system, f appears in the nonlinear coefficients of both the primary system and the absorber, which indicates that it is equivalent to considering the system as being strongly nonlinear or strongly excited. Specifically, Eqs. (7) show that the forcing amplitude modifies linearly the quadratic terms, quadratically the cubic terms and so on. This suggests that, if an optimal set of absorber parameters is chosen for a specific value of f , variations of f will detune the nonlinear absorber, unless the nonlinear coefficients of the primary system and of the absorber undergo a similar variation with f . According to Eqs. (7), this can be achieved by selecting the same mathematical function for the absorber as that of the primary system. When coupled to a Duffing oscillator, the NLTVA should therefore possess a cubic spring:

$$\begin{aligned} q_1'' + 2\mu_1 q_1' + q_1 + \frac{4}{3}\alpha_3 q_1^3 + 2\mu_2 \lambda \epsilon q_2' + \lambda^2 \epsilon q_2 + \frac{4}{3}\epsilon \beta_3 q_2^3 &= \cos \gamma \tau \\ q_2'' + 2\mu_1 q_2' + q_2 + \frac{4}{3}\alpha_3 q_1^3 + 2\mu_2 \lambda (\epsilon + 1) q_2' + \lambda^2 (\epsilon + 1) q_2 + \frac{4}{3}(\epsilon + 1) \beta_3 q_2^3 &= \cos \gamma \tau \end{aligned} \quad (8)$$

where

$$\alpha_3 = \tilde{\alpha}_3 f^2 \quad \text{and} \quad \beta_3 = \frac{3}{4} \frac{f^2 g'''(r)|_{r=0}}{3! m_2 \omega_{n1}^2}. \quad (9)$$

The NLTVA spring should also possess a linear component so that it is effective at low forcing amplitudes where the cubic component of the Duffing oscillator is not activated.

In summary, the proposed nonlinear tuning rule is *to choose the mathematical form of the NLTVA's restoring force so that it is a 'mirror' of the primary system*.

2.4 Definition of the NLTVA parameters

The next objective is to determine the NLTVA parameters, namely ϵ , λ , μ_2 and β_3 . The mass ratio ϵ is chosen according to practical constraints, while the linear parameters λ and μ_2 are determined using Eqs. (2).

Then, the system is solved for a fixed value of $\mu_1 = 0.001$, for different values of ϵ and α_3 , and for a range of excitation frequencies γ encompassing the system's resonances. Starting with weakly nonlinear regimes, i.e., $\alpha_3 > 0$, we seek the value of β_3 , which gives two resonance peaks of equal amplitude. The procedure is repeated for increasing values of α_3 , which allows to consider stronger and stronger nonlinear regimes of motion.

The outcome of this numerical procedure is displayed in Fig. 4 (a). This plot is interesting, because β_3 is almost linearly related to α_3 for the different mass ratios considered, i.e., $\beta_3 \cong a\alpha_3$. This linear relation implies that the nonlinear coefficient of the NLTVA that realizes equal peaks does not depend on forcing amplitude:

$$\beta_3 \cong a\alpha_3 \rightarrow \frac{3}{4} \frac{f^2 g'''(r)|_{r=0}}{3! m_2 \omega_{n1}^2} \cong a \frac{3}{4} \frac{f^2 k_{nl1}}{k_1} \rightarrow g'''(r)|_{r=0} \cong 6a\epsilon k_{nl1} \quad (10)$$

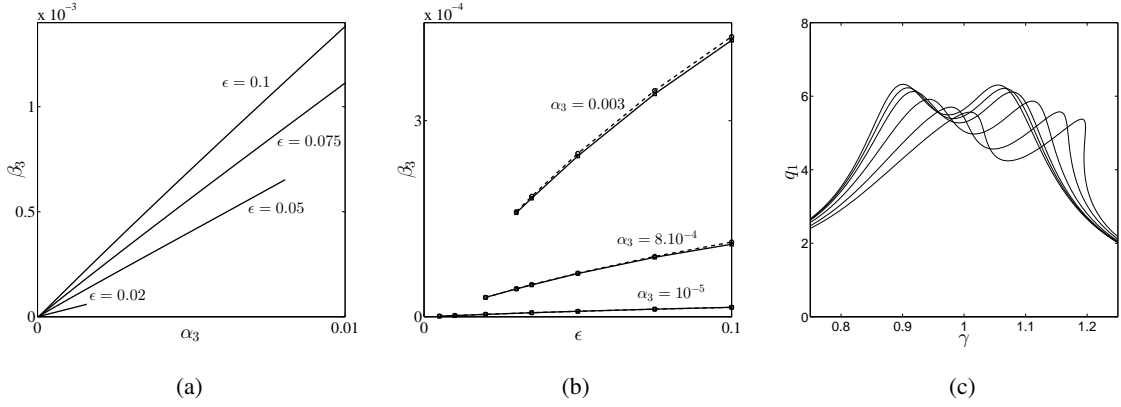


Figure 4: Nonlinear equal-peak method. (a) Values of β_3 realizing equal peaks for increasing α_3 and different ϵ ; (b) values of β_3 realizing equal peaks for increasing ϵ and different α_3 ; the solid line is the result of the numerical computations, and the dashed line is the regression $\beta_3 = 2\alpha_3\epsilon/(1 + 4\epsilon)$. (c) Numerical solution of Eqs. (8) for $\epsilon = 0.05$, $\mu_1 = 0.001$, $\mu_2 = 0.134$, $\lambda = 0.952$. Curves from left to right: $\alpha_3 = 0.0001, 0.0005, 0.001, 0.0025, 0.005, 0.0075$.

The coefficient a is determined by representing β_3 in function of ϵ for different values of α_3 , as in Fig. 4 (b). It turns out that the regression $\beta_3 = 2\alpha_3\epsilon/(1 + 4\epsilon)$ provides an excellent approximation to the numerical results; so $a = 2\epsilon/(1 + 4\epsilon)$.

Equations (8) are now solved considering this analytical expression of β_3 for different values of α_3 and γ , and results are presented in Fig. 4 (c). These results were computed using the path-following algorithm mentioned in Section 2.2. This algorithm provides a very accurate numerical solution to the equations of motion. Fig. 4 (c) shows that the NLTVA can enforce equal peaks in the frequency response q_1 of the Duffing oscillator for values of α_3 ranging from 0.0001 to 0.0075. This result is remarkable in view of the variation of the resonance frequencies. For instance, the first resonance peak occurs at $\gamma = 0.9$ for $\alpha_3 = 0.0001$ and beyond $\gamma = 1$ for $\alpha_3 = 0.0075$. Another interesting observation is that the amplitude of the resonance peaks does not change substantially when α_3 increases, which means that the response of the coupled system is almost proportional to the forcing amplitude, as it would be the case for a linear system. Conversely, Fig. 2 (b) illustrates that the LTVA is strongly detuned for the same parameter values. All these results confirm the efficacy of the proposed NLTVA design.

In summary, given m_1, c_1, k_1 and k_{nl1} for a Duffing oscillator and given a mass ratio ϵ , the NLTVA parameters can be determined using the following analytical formulas:

$$\begin{aligned}
m_2 &= \epsilon m_1 \\
k_2 &= \epsilon k_1 \left[\frac{1}{1 + \epsilon} - \mu_1 \frac{1}{1 + \epsilon} \sqrt{\frac{1}{2(1 + \epsilon)} \left(3 + 4\epsilon - \frac{AB}{2 + \epsilon} \right)} + \mu_1^2 \frac{C_0 - 4(5 + 2\epsilon)AB}{4(1 + \epsilon)^2(2 + \epsilon)(9 + 4\epsilon)} \right]^2 \\
c_2 &= 2\sqrt{k_2 m_2} \left[\sqrt{\frac{3\epsilon}{8(1 + \epsilon)}} + \mu_1 \frac{60 + 63\epsilon + 16\epsilon^2 - 2(3 + 2\epsilon)AB}{8(1 + \epsilon)(2 + \epsilon)(9 + 4\epsilon)} + \right. \\
&\quad \left. \mu_1^2 \frac{C_1(A + B)\sqrt{2 + \epsilon} + C_2(A - B)\sqrt{\epsilon}}{32(1 + \epsilon)(2 + \epsilon)^2(9 + 4\epsilon)^3\sqrt{2\epsilon(1 + \epsilon)}} \right] \\
k_{nl2} &= \frac{2\epsilon^2 k_{nl1}}{(1 + 4\epsilon)}
\end{aligned} \tag{11}$$

These formulas form the basis of a new tuning rule for nonlinear absorbers that may be viewed as a nonlinear generalization of Den Hartog's equal-peak method. We note, however, that there are no invariant points in the nonlinear case. There is thus no complete equivalence with the linear equal-peak method.

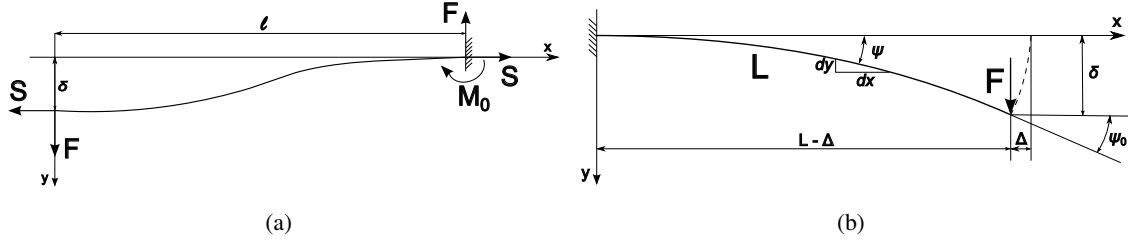


Figure 5: Schematic representation of the beam: (a) cantilever beam, (b) half beam fixed at both ends.

3 Geometrically nonlinear beam models

In this section, analytical formulations for continuous beams are derived in order to build baseline design rules for the NLTVA. It is well-established that slender beams are characterised by nonlinear behaviour, and the challenge is to design their geometrical properties according to the nonlinear load-deflection curve prescribed by the analytical tuning procedure. Realizing with the same beam design prescribed linear and nonlinear stiffness parameters is attempted herein for cubic nonlinearities.

According to the Euler-Bernoulli law, the bending moment M_b at any point of a beam with constant bending stiffness EI is proportional to the change in curvature caused by the action of the load [13]:

$$M_b = EI \frac{d\psi}{ds} \quad (12)$$

where s is curvilinear coordinate along the length of the arc and $\psi(s)$ is the slope at s . In Cartesian coordinates the curvature is expressed as:

$$\frac{d\psi}{ds} = - \frac{d^2y/dx^2}{[1 + (dy/dx)^2]^{3/2}} \quad (13)$$

in which downward deflections are assumed positive and so an increase in x means a decrease in ψ . When the deflection curve is very flat ($dy/dx \ll 1$), the relationship between the bending moment and the curvature can be linearised as

$$M_b = -EI \frac{d^2y}{dx^2}. \quad (14)$$

In conventional engineering applications this approach is justified provided the deflections are small compared with the length of the beam. In the following two different models are presented for the cantilever and doubly-clamped beams using the exact and approximated expressions of the curvature, respectively.

3.1 Cantilever beam

Eq. (12) for a cantilever beam subjected to a tip load, as shown in Figure 5a, can be rewritten as

$$F(L - x - \Delta) = EI \frac{d\psi}{ds}. \quad (15)$$

Differentiating Eq. (15) with respect to s results in

$$\frac{d^2\psi}{ds^2} = - \frac{F}{EI} \cos \psi \quad (16)$$

and integrating with also enforcing null curvature at the loaded end, that is the boundary condition $\left(\frac{d\psi}{ds}\right)_{\psi=\psi_0} = 0$, yields

$$\frac{d\psi}{ds} = \sqrt{\frac{2F}{EI}} (\sin \psi_0 - \sin \psi). \quad (17)$$

If the beam is assumed to be inextensible, the following expression is obtained

$$L = \int_0^{\psi_0} ds = \int_0^{\psi_0} \frac{d\psi}{\sqrt{\frac{2F}{EI} (\sin \psi_0 - \sin \psi)}} \quad (18)$$

that is

$$\sqrt{\frac{FL^2}{EI}} = \int_0^{\psi_0} \frac{d\psi}{\sqrt{2 (\sin \psi_0 - \sin \psi)}}. \quad (19)$$

The problem can be solved using the elliptic integrals of the first and second kinds with the following expression in Legendre's standard form

$$E_1(p^2, \varphi) = \int_0^{\varphi} \frac{dt}{\sqrt{1 - (p \sin t)^2}} \quad (20)$$

$$E_2(p^2, \varphi) = \int_0^{\varphi} \sqrt{1 - (p \sin t)^2} dt \quad (21)$$

Specifically Eq. (19) can be rewritten as follows

$$\sqrt{\frac{FL^2}{EI}} = \int_{\arcsin \frac{1}{p\sqrt{2}}}^{\frac{\pi}{2}} \frac{dt}{\sqrt{1 - (p \sin t)^2}} \quad (22)$$

in which the variable $p = \sqrt{\frac{1 + \sin \psi_0}{2}}$ is introduced in order to bring the right side of Eq. (19) to the standard form of elliptic integrals in Eq. (20). Once the value of the variable p is found by solving the equation

$$\sqrt{\frac{FL^2}{EI}} = E_1\left(p^2, \frac{\pi}{2}\right) - E_1\left(p^2, \arcsin \frac{1}{p\sqrt{2}}\right) \quad (23)$$

then the vertical deflection at the beam tip is given by

$$\delta = \sqrt{\frac{EI}{F}} \left[E_1\left(p^2, \frac{\pi}{2}\right) - E_1\left(p^2, \arcsin \frac{1}{p\sqrt{2}}\right) - 2E_2\left(p^2, \frac{\pi}{2}\right) + 2E_2\left(p^2, \arcsin \frac{1}{p\sqrt{2}}\right) \right] \quad (24)$$

3.2 Doubly-clamped beam

The beam fixed at both ends and subjected to a concentrated load at the centre is a bending problem that admits solution only if a variation of the beam length is allowed. This elongation develops axial forces in the beam in addition to shear forces and bending moments. In order to remain in the elastic range the axial stress cannot exceed a certain value that in turn limits the deflection for the problem under investigation. Therefore, in the following, the approximate expression of the curvature is considered and the longitudinal forces are taken into account. Due to symmetry only the right half of the beam is analysed as represented in Figure 5b, and Eq. (14) can be rewritten as

$$Sy + M_0 - F(L - x) = EI \frac{d^2y}{dx^2}. \quad (25)$$

The boundary conditions for this beam are $y(x = \ell) = \left(\frac{dy}{dx}\right)_{x=0} = \left(\frac{dy}{dx}\right)_{x=\ell} = 0$. The solution of Eq.(25) by imposing the boundary conditions is

$$y = \frac{F}{St} \left[\sinh tx - (1 + \cosh tx) \tanh \frac{t\ell}{2} \right] + \frac{F}{S}(\ell - x) \quad (26)$$

with $t^2 = \frac{S}{EI}$. The deflection at the centre $\delta = y(x = 0)$ depends on the unknown axial load S , so an additional relationship is necessary. It can be obtained from the longitudinal expansion of the beam during deflection. The length of the curve $y = f(x)$ is

$$s = \int_0^\ell \left[1 + \left(\frac{dy}{dx}\right)^2 \right]^{\frac{1}{2}} dx \approx \int_0^\ell \left[1 + \frac{1}{2} \left(\frac{dy}{dx}\right)^2 \right] dx = \ell + \frac{1}{2} \int_0^\ell \left(\frac{dy}{dx}\right)^2 dx \quad (27)$$

in which the approximation of small deflections is used. Since the slope is small, the axial force S can be considered constant along the beam, hence

$$S = AE \frac{\Delta\ell}{\ell} = \frac{AE}{2\ell} \int_0^\ell \left(\frac{dy}{dx}\right)^2 dx \quad (28)$$

in which A is the cross-sectional area of the beam. Finally, combining Eqs. (26) and (28), the applied load F can be expressed as

$$F = \frac{8EI\sqrt{2I/A}}{L^3} u^3 \left[\frac{3}{2} - \frac{1}{2} (\tanh u)^2 - \frac{3 \tanh u}{2u} \right]^{-1/2} \quad (29)$$

in which $u = \sqrt{\frac{L^2 S}{4EI}}$. Once the value of the variable u that generates the applied force F is found from Eq. (29), then the vertical deflection at the centre is given by

$$\delta = \frac{FL^3 (u - \tanh u)}{4EIu^3}. \quad (30)$$

4 Shape optimisation

In this section, a different approach is presented for the NLTVA design. It is based on shape optimisation and provides the geometry of beams for prescribed load-deflection curves, where beam deflections for different prescribed loads are evaluated using a finite element method. An important advantage of this approach is that it can be applied to many different structures and has the potential to achieve complex nonlinear load-deflection curves. The procedure is inspired by a recently-developed optimisation scheme used to design nonlinear materials with prescribed nonlinear properties [17]. In order to take finite strains, rotations and deflections into account, beams are discretised using two-dimensional (2D) geometrically exact beam elements by assuming that the plane cross section of the beam remains plane. The associated strain-deflection relations were derived using the principle of virtual work [14]. Using finite element discretisations, the equilibrium of beams is stated as

$$\mathbf{R} = \mathbf{R}_{\text{int}} - \mathbf{R}_{\text{ext}} = \sum_e \mathbf{r}_{\text{int}} - \mathbf{R}_{\text{ext}} = \mathbf{0} \quad (31)$$

where \mathbf{R} is the residual nodal load vector, \mathbf{R}_{int} and \mathbf{R}_{ext} are the nodal internal and external load vectors, respectively, and \mathbf{r}_{int} is the elemental nodal internal force vector in element, e . Equation (31) is solved using the Newton-Raphson method with the incremental equation given as:

$$\mathbf{K}_t \Delta \mathbf{U} = \mathbf{R} \quad (32)$$

where \mathbf{K}_t is the tangent stiffness matrix, defined as $\mathbf{K}_t = \partial \mathbf{R} / \partial \mathbf{U}$. The nodal displacement vector \mathbf{U} is updated using $\mathbf{U} = \mathbf{U} - \Delta \mathbf{U}$. The detailed calculation of \mathbf{K}_t and \mathbf{R}_{int} can be derived following e.g. [15]

and is not detailed here. Based on the finite element discretisations, element-wise variables, x_e , y_e , and z are introduced to represent the beam geometry, given as

$$w_e = x_e (w_{\max} - w_{\min}) + w_{\min}, h_e = y_e (h_{\max} - h_{\min}) + h_{\min}, l = z (l_{\max} - l_{\min}) + l_{\min} \quad (33)$$

where w_e and h_e are the width and thickness of element, e and l is the total length of the beam, $(\)_{\max}$ and $(\)_{\min}$ represent the maximal and minimal allowed values of corresponding quantities, respectively. The optimisation problem to achieve a prescribed load-deflection curve is formulated to minimize the errors between actual and prescribed deflections for a given load range, stated as

$$\begin{aligned} \min_{x_e, y_e, z} \quad & \max_{i=1, \dots, m} c_i = (\delta(f_i) - \delta^*(f_i))^2 \\ \text{s.t.} \quad & \mathbf{R} = \mathbf{0} \\ & 0 \leq x_e \leq 1, 0 \leq y_e \leq 1, 0 \leq z \leq 1, e = 1, \dots, n \end{aligned} \quad (34)$$

where $\delta(f_i)$ is the actual deflection at the target node for a prescribed load f_i , $\delta^*(f_i)$ is the prescribed deflection for the prescribed load, m is the total target load number in the prescribed load range, n is the total element number. We note that a beam with a uniform width can be designed by assigning a same value to all element-wise design variables x_e , and that a beam with a uniform thickness can be designed by assigning a same value to all element-wise design variables y_e . Using the adjoint methods, the sensitivity of an objective function, c_i with respect to a design variable ϕ is calculated by

$$\frac{\partial c_i}{\partial \phi} = \boldsymbol{\lambda}^T \frac{\partial \mathbf{R}}{\partial \phi} \quad (35)$$

with ϕ as x_e , y_e , or l and $\boldsymbol{\lambda}$ being the adjoint variable vector, which is obtained as

$$(\mathbf{K}_t)^T \boldsymbol{\lambda} = \frac{\partial c}{\partial \mathbf{U}} \quad (36)$$

where \mathbf{K}_t is the tangent stiffness at the converged solution and the operator $(\)^T$ represents the transpose of a matrix. The derivative of the nodal residual vector with respect to a design variable, $\frac{\partial \mathbf{R}}{\partial \phi}$, can be derived directly using the interpolation schemes presented in Eq. (33) and the finite element formulations, and is not presented here for simplification.

Based on the sensitivity analysis, the geometry of beam is iteratively updated using the Method of Moving Asymptotes (MMA) [16]. The finite element analysis and optimisation process are implemented in Matlab and follow the procedure outlined below,

1. Initialize the design variables, x_e , y_e and z .
2. Solve the equilibrium in Eq. (31) for each target load f_i .
3. Calculate the sensitivity of the objective (and possible constraints) with respect to design variables using Eq. (35).
4. Update the design variables using MMA.
5. Repeat step 2–4 until the maximum change of the design variable is smaller than a tolerance or the maximum iteration step is achieved.

5 Results

The design of the mechanical NLTVA is addressed in this section for a nonlinear beam that behaves as a Duffing oscillator around its first resonance. From the reduced nonlinear model of the main structure, the NLTVA parameters are evaluated and then used for the design of different prototypes. At first, cantilever and doubly-clamped beams with uniform cross sections are considered. The beam cross-section profile is then designed using the shape optimisation methodology presented in Section 4.

5.1 Test case description

The primary system is a cantilever beam with a geometrical nonlinearity at its free end. In the set-up, originally proposed in [8], this nonlinear restoring force is due to a more flexible thin beam capable of large deflections. This system can be modelled by using linear beam elements for the main and thin beams and adding a concentrated nonlinear spring at the interface between the two beams, as shown in Figure 6. The geometrical properties of the two beams composing the primary system are listed in Table 1. A numerical

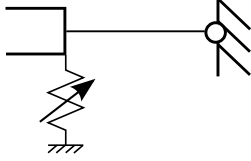


Figure 6: Target location of the primary system.

	Length (m)	Width (m)	Thickness (m)
Main beam	0.70	0.014	0.0140
Thin beam	0.04	0.014	0.0005

Table 1: Geometrical properties of the beams.

model is implemented using 17 Euler-Bernoulli beam elements for the main and the thin beams. Moreover a concentrated nonlinear spring is added at the connection between the two beams to simulate the cubic restoring force due to geometrically nonlinear effects. The coefficient of such nonlinear force was experimentally found equal to $9.9 \times 10^9 \text{ N/m}^3$.

The design procedure proposed in Eqs. (11) is valid for a damped SDOF primary structure. Nevertheless, it can be extended to MDOF structures for which the modal model is evaluated, and a specific mode, e.g. mode k , can be isolated. In such cases, the total mass m_1 of the primary structure should be modified in order to take the modal mass distribution into account. Assuming that the modes are well separated and that in the neighbourhood of ω_k (the frequency of mode k) the response is dominated by mode k , the effective mass of the primary structure with respect to the d -th DOF can be written as

$$m_{1,eff} = \frac{\phi_d^k \mathbf{M} \phi^k}{(\phi_d^k)^2} \quad (37)$$

where ϕ_d^k is the d -th component of the k -th mode shape ϕ^k , and \mathbf{M} is mass matrix of the MDOF main structure. Using the effective mass of the primary structure, an effective mass ratio has now to be considered when Eqs. (11) are evaluated, that is $\epsilon_{eff} = \frac{m_2}{m_{1,eff}}$. The structure under investigation is characterized by well separated normal modes, as can be seen from the natural frequencies and damping ratios summarized in Table 2. The NLTVA design targets the first normal mode and the frequency bandwidth of investigations is limited to [10-60] Hz, where the system response is dominated by this mode. The physical mass of the beam m_{beam} is 1.1 kg and the effective mass in Table 2 is calculated with respect to the degree of freedom where the nonlinearity is attached, that is also the selected location for NLTVA. The mechanical design of the

Mode	Natural frequency (Hz)	Damping ratio (%)	Effective mass (kg)
1	31.63	0.23	0.30
2	147.1	0.08	0.28
3	407.1	0.12	0.29

Table 2: Modal parameters of the first three modes of the main structure.

Young Modulus	Density	minimum thickness
1950 MPa	1175 kg/m ³	0.5 mm

Table 3: Polyjet Digital ABS material properties.

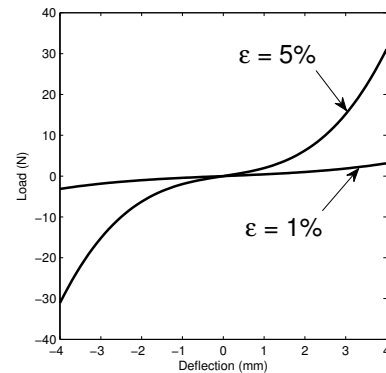


Figure 7: NLTVA load-deflection functions.

NLTVA is addressed in the following sections for two different test cases with physical mass ratios between the absorber and the host structure, i.e. $\epsilon_{phys} = m_2/m_{beam}$ equal to 1% and 5%. This condition directly sets the mass of the mechanical NLTVA equal to 1.1×10^{-2} kg and 5.5×10^{-2} kg, for the two test cases respectively. Therefore, the linear and nonlinear stiffness coefficients provided by the NLTVA tuning rule in Section 5.2 are used to built the static load-deflection objective function given by

$$f(\delta^*) = k_{nl}\delta^{*3} + k_2\delta^* \quad (38)$$

and represented in Figure 7 for deflection range of 4 mm. The proposed design procedure assumes that the mass of the nonlinear beam is negligible with respect to the prescribed overall mass of the absorber m_2 . Therefore, when a lumped mass is added where the deflection δ^* is evaluated, the nonlinear beam behaves as a SDOF NLTVA connected to the host structure. Herein, the dimensioning of the damping is not performed, and it is assumed that the selection of a proper material could address this requirement in future. In Sections 3 and 4 is shown that not only the beams' geometrical dimensions affect the load-deflection curves, but also the material properties, i.e. the Young modulus, come into play. The important progress in 3D printing technology makes easy the manufacturing of any uniform and modulated, cantilever or doubly-clamped beams. Therefore hereinafter, the NLTVA is assumed to be manufactured using a Statasys 3D printer with the Polyjet Digital ABS material. This material is specifically designed to simulate engineering plastics with high strength, and it also offers the possibility to create thin-walled parts. The mechanical properties are summarized in Table 3.

5.2 NLTVA parameters

The values obtained for the NLTVA parameters using Eqs. (11) with $\epsilon = \epsilon_{eff}$ and $m_1 = m_{1,eff}$ for the first mode of Table 2 are given in Table 4, for physical mass ratios ϵ_{phys} of 1% and 5% (corresponding to effective mass ratio ϵ_{eff} of 3.7% and 18%, respectively). For this configuration however, as it will be shown later in this section, the two peak amplitudes on the frequency response are not exactly equal. This can first be

		Physical mass ratio	Physical mass ratio
		$\epsilon_{phys} = 1\%$	$\epsilon_{phys} = 5\%$
k_2	Analytical [N/m]	405.455	1552.19
	Exact [N/m]	407.685	1583.88
	Rel. error [%]	0.55	2.00
c_2	Analytical [Ns/m]	0.4901	4.4783
	Exact [Ns/m]	0.4944	4.6012
	Rel. error [%]	0.87	2.67
k_{nl2}	Analytical [N/m ³]	2.33967×10^7	3.86449×10^8
	Exact [N/m ³]	2.3585×10^7	3.86794×10^8
	Rel. error [%]	0.80	0.09

Table 4: NLTVA parameters for the nonlinear primary structure under investigation. Analytical values from Eqs. (11), exact values for equal peaks, and relative errors with respect to the exact values.

explained by the fact that the NLTVA design procedure was applied on a SDOF approximation of the beam through its first mode, although other modes could participate to the response of the structure. Moreover, another source of error comes from the fact that k_{nl2} in Eqs. (11) is an approximation of the exact value through a linear regression.

The values of the NLTVA parameters giving exactly equal resonance peaks can be computed by trial-and-error with the parameters obtained from the analytical expressions as initial guess. Forcing amplitudes of 2.08 N and 7.5 N are chosen for the tuning of k_{nl2} , for the configurations with physical mass ratio of 1% and 5%, respectively. These exact values are also given in Table 4, together with the relative errors made with the analytical expressions. One observes that the relative errors are almost negligible from the point of view of the practical realization of the absorber, which validates the procedure described in Section 5.1 for

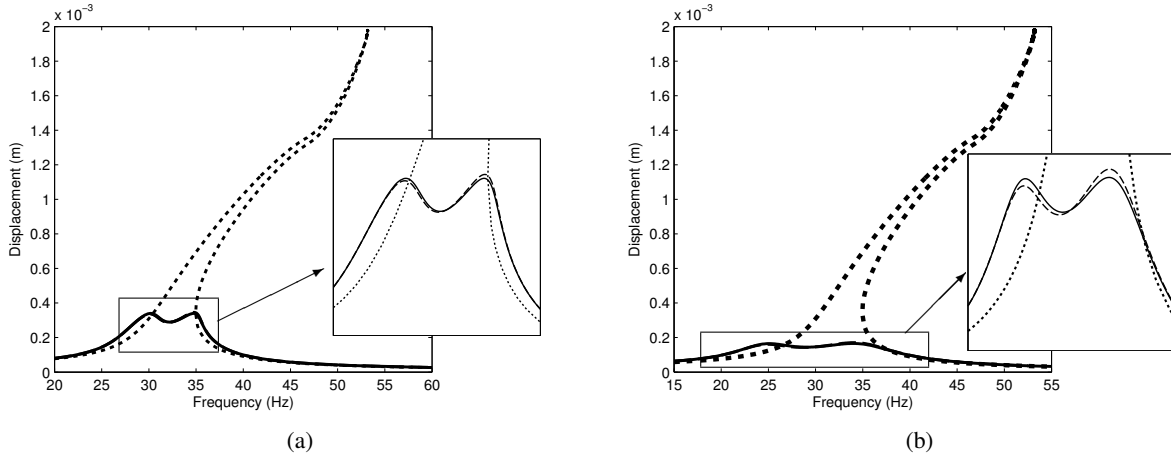


Figure 8: Frequency response of the vertical displacement at the tip of the clamped beam, without NLTVA (dotted line) and with NLTVA attached, for a forcing amplitude $F = 2.08$ N. The solid line represents the configuration with an NLTVA exactly tuned for equal resonance peaks, and the dashed line represents the configuration with an NLTVA tuned with the analytical expression. (a) Physical mass ratio $\epsilon_{phys} = 1\%$; (b) Physical mass ratio $\epsilon_{phys} = 5\%$.

the SDOF approximation. Figures 8(a) and (b) represent the frequency response of the vertical displacement at the tip of the beam, when NLTVA with mass ratio $\epsilon_{phys} = 1\%$ and 5% are attached, respectively, and for a forcing amplitude $F = 2.08$ N. The responses for the configuration of the NLTVA giving exactly equal resonance peaks, and the configuration of the NLTVA obtained from the application of Eqs. (11) to the nonlinear beam, are both given. Interestingly enough, one notices that the peaks obtained from the analytical approximation of the parameters are not equal, but reasonably close. The performance of the NLTVA also improves for higher mass ratio, as expected. For a more global evaluation of the performance of the absorbers, Figures 9 (a) and (b) show the amplitude of the resonance peaks at the tip of the beam as a function of the forcing amplitude F , for two different mass ratios $\epsilon_{phys} = 1\%$ and 5% , respectively. For each mass ratio, two configurations are considered: the NLTVA, and the linear tuned vibration absorber (LTVA), which has the same parameters as the NLTVA but without nonlinear stiffness. First, one can verify that the absorbers with 5% mass ratio performs better than the absorber with 1% mass ratio. It is also interesting to notice that, for both mass ratios, the two peak amplitudes for the configurations with NLTVA remain equal for a large forcing amplitude interval, and smoothly start to diverge from each other at $F = 4$ N in Figure 9 (a) and at 10 N in Figure 9 (b). In this interval, the amplitude is almost linearly related to forcing amplitude, as if the system would obey the superposition principle. This result is unexpected in view of the strongly nonlinear regimes investigated. It therefore seems that adding a properly chosen nonlinearity to an already nonlinear system can somehow linearise the dynamics of the coupled system. As a comparison, the peak amplitudes for the systems with LTVA rapidly diverge from each other. Moreover, in Figure 9 (a) one observes that the LTVA and the NLTVA with $\epsilon_{phys} = 1\%$ suddenly get detuned around forcing amplitudes $F = 2.08$ N and 7.5 N, respectively. This justifies why one considered these forcing amplitudes for the tuning of k_{nl2} for both configurations. It can however be shown that the value F at which the tuning is realized has a negligible influence on the value of k_{nl2} , as already suggested in Figures 9 (a) and (b) by the fact that the equal peak criterion is verified in a large forcing amplitudes interval.

5.3 Mechanical design of the NLTVA with continuous beams

The geometrically nonlinear models of cantilever and doubly-clamped beams described in Section 3 are considered to dimension the mechanical NLTVA. The nonlinear relationships given in Eqs. (24) and (30) cannot be easily inverted, but they can be implemented for a specific beam to have load-deflection functions defined

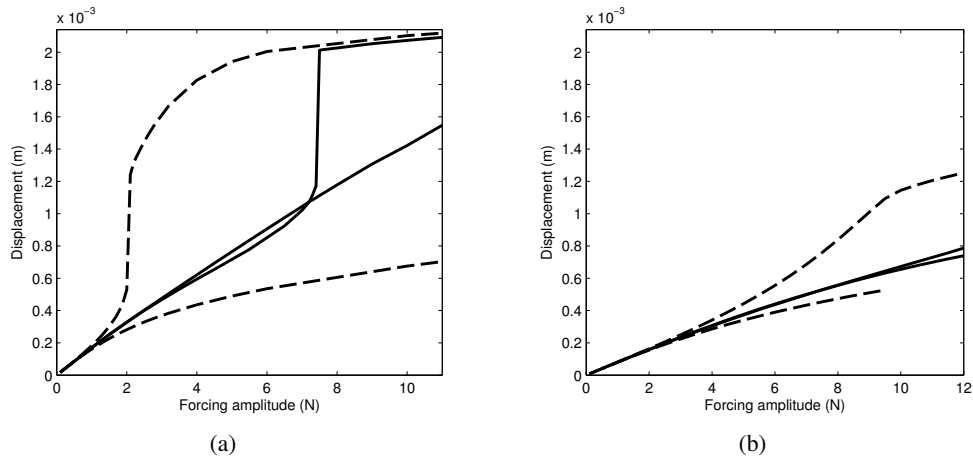


Figure 9: Performance of the NLVTA (solid lines) and the LTVA (dashed lines) for increasing forcing amplitudes F . Amplitude of the resonance peaks at the tip of the beam. (a) Physical mass ratio $\epsilon_{phys} = 1\%$; (b) Physical mass ratio $\epsilon_{phys} = 5\%$.

by points in a defined deflection interval. Therefore, the geometrical dimensions of the beam with rectangular cross section can be selected in terms of length, width and thickness such that the load-deflection functions closely match the objective function in Eq. (38). The analytical and the exact values of the coefficients given in Table 4 are used in Eq. (38) to define the objective functions for the two physical mass ratios of 1% and 5%. The dimensions of the cantilever and doubly-clamped beams for all the test cases are summarized in Table 5.

geometrical parameter		cantilever		doubly-clamped	
		$\epsilon_{phys} = 1\%$	$\epsilon_{phys} = 5\%$	$\epsilon_{phys} = 1\%$	$\epsilon_{phys} = 5\%$
length (mm)	Analytical	6.47	3.17	232.93	67.37
	Exact	6.46	3.20	232.93	67.57
width (mm)	Analytical	1.00	1.00	4.00	4.00
	Exact	1.00	1.00	4.00	4.00
thickness (mm)	Analytical	0.64	0.49	3.45	1.50
	Exact	0.64	0.50	3.45	1.51

Table 5: NLTVA dimensions using uniform cantilever and doubly-clamped beams and stiffness coefficients as coming from the analytical and the exact solutions for physical mass ratios equal to 1% and 5%.

As argued in the previous section, the geometrical dimensions for all the beams in Table 5 are practically not affected by the small error on the stiffness coefficients. In fact the differences between the values achieved with the analytical formulas and those related to the exact parameters are within the manufacturing margin of errors. Although all the solutions in Table 5 could in principle be used as NLTVA, it has to be noted that the cantilever designs are too tiny. Their small dimensions still satisfy the manufacturing limitations, but it would be hard to handle beams length 6.5 mm and 3.2 mm, and properly attach the corresponding lumped masses of 1.1×10^{-2} kg and 5.5×10^{-2} kg, for the two test cases respectively.

The objective functions computed using the exact coefficients are represented in Figure 10 together with the load-deflection curves of the cantilever and doubly-clamped beams having the dimensions of Table 5. If these curves are fitted using a function analogous to Eq. (38) some useful and accurate design formulas can be extracted. Specifically, for the cantilever beam the nonlinear and linear coefficients are given by

$$k_{nl2} \approx 3.44 \frac{EI}{L^5}, \quad k_2 = 3 \frac{EI}{L^3} \quad (39)$$

It is worth remarking that the linear coefficient is consistent with the linear theory of the Euler-Bernoulli cantilever beam subjected to a tip load. Although the coefficients in Eqs. (39) define an approximated load-

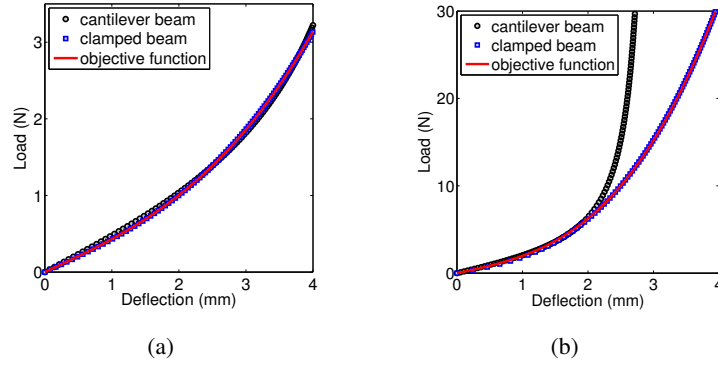


Figure 10: Load-deflection functions of the cantilever and doubly-clamped beams for different configurations compared with the objective functions. (a) Physical mass ratio $\epsilon_{phys} = 1\%$; (b) Physical mass ratio $\epsilon_{phys} = 5\%$.

deflection function for the cantilever beam, their analysis suggests important guidelines in the selection of the geometrical characteristics of the NLTVA mechanical realization. One observes that for given coefficients k_{nl2} and k_2 , also their ratio is set and as a consequence the length of the beam comes from the relationship $k_{nl2}/k_2 = 1.15L^2$. This explains the limitation in using cantilever beams for the analysed test case; the constraint on the length cannot be overcome and a tiny prototype results as shown in table 5. Moreover, it can be noted that in Figure 10 the curve related to the cantilever beam for $\epsilon_{phys} = 5\%$ strongly diverges from the objective function for deflections larger than 2 mm, and this is because its length is of only 3.2 mm. Similar analysis can be performed on the doubly-clamped beams and the nonlinear and linear coefficients can be extrapolated by fitting the load-deflection functions. This results in

$$k_{nl2} \approx \pi^4 \frac{EA}{8L^3}, \quad k_2 = 2\pi^4 \frac{EI}{L^3} \quad (40)$$

As for the cantilever configuration, the linear term is in agreement with the linear theory of the doubly-clamped beam when the axial forces are neglected. It is interesting to observe that the coefficient of the nonlinear term depends on the axial stiffness of the beam EA , as already achieved in [18]. Therefore, in this configuration the cross section is the geometrical parameter driving the design. In fact, the ratio between the nonlinear and the linear coefficients does not depend any more on the beam length, but relates the area and the momentum of inertia of the cross section. For rectangular cross sections of thickness t this relationship is $k_{nl2}/k_2 = \frac{2}{t^2}$. In the analysed test case, this constraint suggests reasonable results and the designs of the doubly-clamped beams can be manufactured by 3D printing using the dimensions given in Table 5.

5.4 Optimised solutions for the NLTVA mechanical design

In this section, we optimise the geometries of the cantilever and doubly-clamped beams using Eq. (34) to achieve the prescribed nonlinear load-deflection curves represented in Figure 7 as given by the exact values in Table 4. In the first part, we aim at designing cantilever beams. In the second part, we aim at designing doubly-clamped beams.

Tables 6 and 7 present the optimised cantilever beams for load-deflection curves related to physical mass ratios equal to 1% and 5%, respectively. When 2D geometrically exact beam elements implemented as in [14] are used, the objective functions are not properly fitted. Better performances are achieved by allowing modulated thickness or width. Among all the designs, the optimised beams with modulated width and thickness can identically achieve the prescribed load-deflection curves related to physical mass ratios equal to 1% and 5%. For the same optimisation parameters, the optimised beams for 1% mass ratio exhibit smaller length than ones for 5% mass ratio. However, it is noted that the dimensions of the optimised beams are very





	uniform design	modulate width	modulate thickness	modulate width& thickness
length (mm)	5.78	7.50	11.22	11.89
width (mm)	0.64	[0.20, 3.57]	0.20	[0.35, 1.55]
				
thickness (mm)	0.64	0.65	[0.20, 1.52]	[0.35, 1.56]
				

Table 6: Optimised cantilever beam for nonlinear load-deflection curve related to 1% physical mass ratio.





	uniform design	modulate width	modulate thickness	modulate width& thickness
length (mm)	2.79	4.00	4.50	5.28
width (mm)	0.52	[0.20, 5.82]	0.20	[0.20, 1.45]
				
thickness (mm)	0.52	0.58	[0.20, 1.15]	[0.20, 1.45]
				

Table 7: Optimised cantilever beam for nonlinear load-deflection curve related to 5% physical mass ratio.


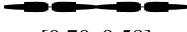


	uniform design	modulate width	modulate thickness	modulate width& thickness
length (mm)	244.81	305.64	255.94	254.62
width (mm)	4.46	[2.31, 19.69]	2.63	[0.71, 9.31]
				
thickness (mm)	3.47	3.99	[2.63, 9.76]	[0.70, 9.58]
				

Table 8: Optimised doubly-clamped beam for nonlinear load-deflection curve related to 1% physical mass ratio





	uniform design	modulate width	modulate thickness	modulate width& thickness
length (mm)	59.66	40.19	64.13	61.61
width (mm)	2.09	[0.20, 5.571]	2.51	[0.54, 3.19]
				
thickness (mm)	1.72	1.51	[0.71, 2.51]	[0.54, 3.24]
				

Table 9: Optimised doubly-clamped beam for nonlinear load-deflection curve related to 5% physical mass ratio.

small and all the optimised cantilever beams possess dimensions smaller than 0.5 mm in both the width and thickness. Hence, it is difficult to manufacture them using 3D printing.

In the second part, the doubly-clamped beams are optimised to achieve the prescribed load-deflection curves. Tables 8 and 9 present the optimised beams for physical mass ratios equal to 1% and 5%, respectively. Same as in the previous case, the 5% mass ratio leads to much smaller beams, compared to the case with 1%. It is noted that all the optimised doubly-clamped beams exhibit much larger dimensions than the optimised cantilever beams, and therefore can be manufactured using the 3D printer.

5.5 Discussion

Thanks to the procedure summarised in Figure 1, effective NLTVA prototypes can be designed when the primary structure behaves as a Duffing oscillator around the resonance of interest. Combining Eqs. (11) with Eqs. (39 – 40), the geometrical dimensions of uniform cantilever and doubly-clamped beams can be derived analytically as functions of only the linear and nonlinear stiffness of the primary system (k_1 and k_{nl1} , respectively) and the mass ratio ϵ . The design procedure is therefore greatly simplified as represented in Figure 11. The beams can then be directly manufactured using 3D printing.

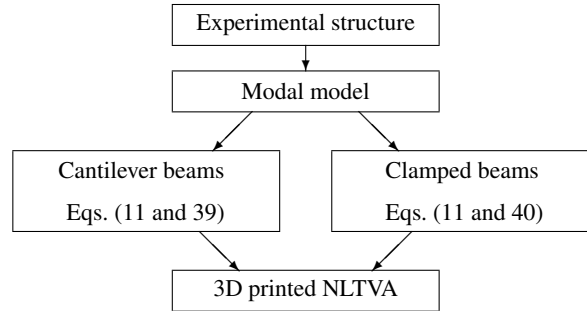


Figure 11: Diagram of the design procedure.

Conversely, the implementation of the shape optimisation procedure cannot be further simplified. However, its flexibility with regard to the pre-assigned load-deflection curve allows the design of many different mechanical NLTVA. The application on discretised beams provides different designs with modulated width and/or thickness. Therefore, this approach, combined with the 3D printing technology, is very promising for the practical application of the NLTVA to engineering structures.

6 Concluding remarks

A practical design procedure of a new nonlinear tuned vibration absorber is described in the present paper. The analytical formulation proves that the NLTVA is capable of mitigating the vibrations of nonlinear systems for a large range of forcing amplitudes. Several mechanical designs are proposed using continuous and discretised cantilever and doubly-clamped beams. These designs, suitable to be manufactured by 3D printing, are derived by imposing the nonlinear load-deflection functions prescribed by the analytical formulation. The application of the methodology to a nonlinear MDOF main structure shows that the NLTVA can be effectively used for mitigating one specific resonance.

Acknowledgements

The authors Chiara Grappasonni, Giuseppe Habib, Thibaut Detroux and Gaëtan Kerschen would like to acknowledge the financial support of the European Union (ERC Starting Grant NoVib 307265), the authors Fengwen Wang and Jakob S. Jensen would like to acknowledge the ERC Starting Grant (INNODYN).

References

- [1] J.P. Den Hartog, *Mechanical Vibrations*, McGraw-Hill, New York (1934).

- [2] J. Ormondroyd, J.P. Den Hartog, *The Theory of the Dynamic Vibration Absorber*, Transactions of ASME, Vol. 50, pp. 9-22, (1928).
- [3] J.E. Brock, *A Note on the Damped Vibration Absorber*, Journal of Applied Mechanics, Vol. 13, pp. A284, (1946).
- [4] T. Asami, O. Nishihara, *Closed-form Exact Solution to H_∞ Optimization of Dynamic Vibration Absorbers (Application to Different Transfer Functions and Damping Systems)*, Journal of Vibration and Acoustics, Vol. 125, pp. 398-405, (2003).
- [5] T. Asami, O. Nishihara, A.M. Baz, *Analytical Solutions to H_∞ and H_2 Optimization of Dynamic Vibration Absorbers Attached to Damped Linear Systems*, Journal of Vibration and Acoustics, Vol. 124, pp. 284-295, (2002).
- [6] S.S. Oueini, A.H. Nayfeh, *Analysis and application of a nonlinear vibration absorber*, Journal of Vibration and Control, Vol. 6, No. 7, pp. 999-1016, (2000).
- [7] A.F. Vakakis, O. Gendelman, L.A. Bergman, D.M. McFarland, G. Kerschen, Y.S. Lee, *Nonlinear Targeted Energy Transfer in Mechanical and Structural Systems*, Springer (2009).
- [8] F.Thouverez, *Presentation of the ECL benchmark*, Mechanical Systems and Signal Processing, Vol. 17, No. 1, pp. 195-202, (2003).
- [9] H. Frahm, *Device for Damping Vibrations of Bodies*, US No. Patent 989958, (1909).
- [10] J.Q. Sun, M.R. Jolly, M.A. Norris, *Passive, Adaptive, and Active Tuned Vibration Absorbers - A Survey*, Journal of Mechanical Design, Vol. 117, pp. 234-242, (1995).
- [11] M. Peeters, R. Vigué, G. Sérandour, G. Kerschen, J.C. Golinval, *Nonlinear Normal Modes, Part II: Toward a Practical Computation using Numerical Continuation*, Mechanical Systems and Signal Processing, Vol. 23, pp. 195-216, (2009).
- [12] R.E. Roberson, *Synthesis of a Nonlinear Dynamic Vibration Absorber*, Journal of the Franklin Institute, Vol. 254, pp. 205-220, (1952).
- [13] R.Frisch-Fay, *Flexible bars*, Butterworths ed., London (1962).
- [14] E. Reissner, *On one-dimensional finite-strain beam theory: the plane problem*, Zeitschrift für angewandte Mathematik und Physik ZAMP, Vol. 23, pp. 795-804, (1972).
- [15] P. Wriggers, *Nonlinear finite element methods*, Vol. 4, Springer, Berlin (2008).
- [16] K. Svanberg, *The method of moving asymptotes: a new method for structural optimization*, International journal for numerical methods in engineering, Vol. 24, No. 2, pp. 359-373, (1987).
- [17] F. Wang, O. Sigmund, J.S. Jensen, *Design of materials with prescribed nonlinear properties*, Journal of the Mechanics and Physics of Solids, Vol. 69, pp. 156-174, (2014).
- [18] S.D. Senturia, *Microsystem design*, Vol. 3, Kluwer academic publishers, Boston (2001).